

# On singular probability densities generated by extremal dynamics

Guilherme J. M. Garcia\* and Ronald Dickman†  
Departamento de Física, Instituto de Ciências Exatas  
Universidade Federal de Minas Gerais, Caixa Postal 702  
CEP 30123-970, Belo Horizonte - Minas Gerais, Brazil  
(November 2, 2018)

## Abstract

Extremal dynamics is the mechanism that drives the Bak-Sneppen model into a (self-organized) critical state, marked by a singular stationary probability density  $p(x)$ . With the aim of understanding of this phenomenon, we study the BS model and several variants via mean-field theory and simulation. In all cases, we find that  $p(x)$  is singular at one or more points, as a consequence of extremal dynamics. Furthermore we show that the extremal barrier  $x_i$  always belongs to the ‘prohibited’ interval, in which  $p(x) = 0$ . Our simulations indicate that the Bak-Sneppen universality class is robust with regard to changes in the updating rule: we find the same value for the exponent  $\pi$  for all variants. Mean-field theory, which furnishes an exact description for the model on a complete graph, reproduces the character of the probability distribution found in simulations. For the modified processes mean-field theory takes the form of a functional equation for  $p(x)$ .

PACS: 05.65.+b, 02.30.Ks, 05.40.-a, 87.10.+e

keywords: extremal dynamics; Bak-Sneppen model; mean-field theory; functional equations; universality

\* Electronic address: gjmg@fisica.ufmg.br

† Electronic address: dickman@fisica.ufmg.br

Corresponding author: Ronald Dickman  
telephone: 55-31-3499-5665  
FAX: 55-31-3499-5600

## I. INTRODUCTION

The Bak-Sneppen (BS) model was proposed as a possible explanation of mass extinctions observed in the fossil record [1], and was recently adapted to model experimental data on bacterial populations [2,3]. Independent of its biological interpretation, the model has attracted much attention as a prototype of self-organized criticality (SOC) under extremal dynamics [4,5]. The model has been studied through various approaches, including simulation [6–8], theoretical analysis [9–11], probabilistic analysis (run time statistics) [12,13], renormalization group [14,15], field theory [16] and mean-field theory [4,5,17]. Some variants have been proposed, for example the anisotropic BS model [18,19]. In this paper, we study the consequences of extremal dynamics, using mean-field theory and simulation. With this aim, we propose variants of the model and analyse how varying the updating rule affects the stationary probability density and the critical behaviour.

In the evolutionary interpretation of the BS model, each site  $i$  represents a “niche” occupied by a single species, and bears a real-valued variable  $x_i$  representing the “fitness” of this species. (In the present context “fitness” denotes a propensity to resist extinction: if  $x_i > x_j$  then species  $j$  goes extinct before  $i$ , so that  $x_i$  may be termed a “barrier to extinction”.) At each step the site with the smallest  $x_i$ , and its nearest neighbors, are replaced with randomly chosen values. The replacement of the neighboring variables with new random values may be interpreted as a sudden unpredictable change in fitness when a nearby niche (which might have borne a predator, or a food source for the species in question), is suddenly colonized by a new species. Selection, at each step, of the global minimum of the  $\{x_i\}$  (“extremal dynamics”) represents a highly nonlocal process, and would appear to require an external agent with complete information regarding the state of the system at each moment. Applications of the model in evolution studies are reviewed in [20].

In the original updating rule, neighbors are randomly affected by the extinction of an interacting species. There is no *a priori* reason to expect that evolution should obey this specific rule on a specific lattice. Thus, we ask: what happens if the extinction of the least adapted species favors (or prevents) the extinction of other species? Moreover, what is the signature of extremal dynamics that can, in principle, allow us to recognize it in the real world?

Due to extremal dynamics, the BS model exhibits scale invariance in the stationary state, in which several quantities display power-law behaviour [1]. Simulations show that the stationary distribution of barriers follows a step function, being zero (in the infinite-size limit) for  $x < x^* \simeq 0.66702(8)$  [6]. Relaxing the extremal condition leads to a smooth probability density and loss of scale invariance [4,5].

A striking feature of the BS model is that a simple updating rule leads to a singular stationary probability density  $p(x)$ . An intriguing question therefore arises, as to how changes in the updating rule affect this density, an issue that

has not, to our knowledge, been investigated previously. In this work we examine the consequences of rules in which one or more sites are updated according to  $x \rightarrow x' = f(x)$ , instead of being replaced by a random number. (Here  $f$  maps the interval  $[0,1]$  to itself.) We find that this can provoke dramatic changes in the stationary probability density. In the extremal dynamics limit, the variant models belong to the same universality class as the original. We find that the hallmarks of extremal dynamics are that i) the stationary probability density is singular, and ii) with probability one, the extremal  $x_i$  (i.e., the next variable to be updated) belongs to the ‘prohibited’ region in which  $p(x) = 0$ . Using a two-site mean-field approximation, we also find evidence that nontrivial correlations are restricted to the prohibited region.

The balance of this paper is organized as follows. Section II introduces the models, which are then analyzed using mean-field like approaches in Sec. III. In Sec. IV we present simulation results, and summarize our conclusions in Sec. V.

## II. MODELS

The Bak-Sneppen [1] model is a discrete-time Markov process on a  $d$ -dimensional lattice of  $L^d$  sites, with periodic boundaries. At each site we define a real-valued variable  $x_i(0)$ . Initially, these variables are independently assigned random values uniform on  $[0,1]$ . At time 1, the site  $m$  bearing the minimum of all the numbers  $\{x_i(0)\}$  is identified, and it, along with its  $2d$  nearest neighbors, are given new random values, again drawn independently from the interval  $[0,1]$ . (In the one dimensional case considered here this amounts to:  $x_m(1) = \eta$ ,  $x_{m+1}(1) = \eta'$ , and  $x_{m-1}(1) = \eta''$ , where  $\eta$ ,  $\eta'$ , and  $\eta''$  are independent and uniformly distributed on  $[0,1]$ ; for  $|j - m| > 1$ ,  $x_j(1) = x_j(0)$ .) At step 2 this process is repeated, with  $m$  representing the site with the global minimum of the variables  $\{x_i(1)\}$ , and so on. In the *random neighbor* version of the model, the process is realized on a complete graph (all sites are considered neighbors); two randomly selected sites are updated in addition to the minimum  $m$ .

We now define three modified Bak-Sneppen models, that differ from the original only in the way that the barriers  $x_i$  evolve. In one, the site  $M$  bearing the *maximum* of the  $\{x_i\}$  is replaced with a random number  $\eta$  and the two nearest neighbors are replaced with their own *square roots*:  $x_M(t+1) = \eta$  and  $x_{M\pm 1}(t+1) = \sqrt{x_{M\pm 1}(t)}$ . We shall refer to this as the ‘radical’ variant. In the second variant, the site with the maximum value is replaced by its own value *squared*, while its two nearest neighbors receive random numbers  $\eta$  and  $\eta'$ :  $x_M(t+1) = [x_M(t)]^2$ ,  $x_{M+1}(t+1) = \eta$ , and  $x_{M-1}(t+1) = \eta'$ . This will be called the ‘centered square’ version. Finally, we define a ‘peripheral square’ variant, in which one of the nearest neighbors of  $M$  is squared, while  $M$  and its other neighbor are replaced with random numbers:  $x_{M'}(t+1) = [x_{M'}(t)]^2$ ,  $x_M(t+1) = \eta$  and  $x_{M''}(t+1) = \eta'$ . (Here  $M' = M + \sigma$  and  $M'' = M - \sigma$ ,

where  $\sigma$  is a random variable that assumes values of +1 and -1 with equal probability.)

The motivation for studying these variants is twofold. First, the Bak-Sneppen model is notable for exhibiting a singular stationary probability density, and it is of interest to examine the effect of changes in the dynamical rule on this density and on the critical behavior. If we introduce a deterministic function  $f(x)$  as part of the updating rule, it is desirable that  $f$  map the interval  $[0,1]$  to itself, making functions of the form  $f(x) = x^\alpha$  a natural choice. In this context we note that the variants feature what may be called ‘migration’, that is, the systematic movement of certain variables  $x_i$  within the interval  $[0,1]$ . In the radical variant the migration is from the populated region (smaller  $x$ ) to the ‘excluded’ region (larger  $x$ ), whereas in the square versions migration occurs in the opposite direction.

Secondly, the variants admit interpretation as evolutionary processes. (In the modified models, we have for convenience defined the site with the maximum variable as the most vulnerable, so that small  $x_i$  now corresponds to high fitness.) In the radical variant, replacement of the least-fit species provokes a reduction in the fitness of its neighbors, without leading to their immediate extinction. Thus, some memory of the fitness of the neighboring species is retained. The radical variant therefore seems a plausible modification of the original model, in the biological context. In the peripheral square variant the extinction of the least-fit species provokes extinction of one neighbor, and increased fitness of the other. Finally, in the centered-square variant,  $x_M \rightarrow x_M^2$  represents an increase in the fitness of the least viable element of the system, while its neighbors go extinct.

### III. MEAN-FIELD THEORY

#### A. Original Model

We develop mean-field approximations for the original and modified models, along the lines of Refs. [4] and [5]. To begin, we relax the extremal condition introducing a flipping rate of  $\Gamma e^{-\beta x_i}$  at site  $i$ , where  $\Gamma^{-1}$  is a characteristic time, irrelevant to stationary properties, and which we set equal to one ( $\Gamma = 1$ ). Call this regularized system the ‘finite-temperature’ model. The extremal dynamics of the original model is recovered in the zero-temperature limit,  $\beta \rightarrow \infty$ .

Consider the probability density  $p(x)$ . In the finite-temperature version of the original model,  $p(x)$  satisfies

$$\frac{dp(x,t)}{dt} = -e^{-\beta x}p(x,t) - 2 \int_0^1 e^{-\beta y}p(x,y,t)dy + 3 \int_0^1 e^{-\beta y}p(y,t)dy \quad , \quad (1)$$

where  $p(x,y,t)$  is the joint density for a pair of nearest-neighbor sites and  $p(y,t)$  is the one-site marginal density. Invoking the mean-field factorization  $p(x,y) = p(x)p(y)$  (we suppress the time argument from here on), we find:

$$\frac{dp(x)}{dt} = -[e^{-\beta x} + 2I(\beta)]p(x) + 3I(\beta) \quad , \quad (2)$$

where

$$I(\beta) \equiv \int_0^1 e^{-\beta y} p(y) dy \quad , \quad (3)$$

represents the overall flipping rate. Eq. (2) is a nonlinear equation for  $p$ , in which the density at  $x$  is coupled to  $p$  at all other arguments via  $I(\beta)$ .

In the stationary state we have

$$p(x) = \frac{3I}{2I + e^{-\beta x}} \quad . \quad (4)$$

Multiplying by  $e^{-\beta x}$  and integrating over the range of  $x$ , we find

$$I(\beta) = (e^{2\beta/3} - 1)/[2e^\beta(1 - e^{-\beta/3})], \quad (5)$$

and thus

$$p_{st}(x) = \frac{3}{2} \frac{1 - e^{-2\beta/3}}{1 - e^{-2\beta/3} + e^{-\beta x}(e^{\beta/3} - 1)} \quad . \quad (6)$$

This solution is plotted for various  $\beta$  values in Fig. 1.

In the limit  $\beta \rightarrow \infty$  the solution becomes a step function:

$$p_{st}(x) = \frac{3}{2} \Theta(x - 1/3) \Theta(1 - x) \quad . \quad (7)$$

Thus the mean-field approach correctly predicts a step-function singularity for the probability density, although it places the critical barrier at  $x^* = 1/3$ , whereas it actually falls at 0.66702(8) [6]. On the other hand, the slightest relaxation of the extremal condition destroys the singularity [5], since  $p(x)$  is a smooth function for  $\beta < \infty$ . The rate of convergence to the step-function is generally exponential with  $\beta$ , away from the discontinuity. The curves for various  $\beta$  values exhibit an approximate crossing near  $x = 1/3$ . The derivative at this point however diverges only linearly with  $\beta$ :  $(dp_{st}/dx)_{x=1/3} \simeq 3\beta/8$  for large  $\beta$ .

Using Eq. (2), we find, in the limit of large  $\beta$ , that the relaxation time for a small disturbance from the stationary solution grows  $\sim e^{\beta/3}$ . (By ‘small’ we mean  $I(\beta) \simeq e^{-\beta/3}/2$ .)

The following observation will prove useful in the discussion of the modified models. If we assume that, in the limit  $\beta \rightarrow \infty$ ,  $p_{st}(x)$  is identically zero for  $x < x^*$ , and that  $p_{st} \geq C > 0$  on some interval  $[x^*, a]$  (in other words, the density suffers a jump discontinuity at  $x^*$ ), then  $I = \int_0^1 e^{-\beta y} p(y) dy \sim e^{-\beta x^*}$  and so  $e^{-\beta x}/I \sim e^{-\beta(x-x^*)} \rightarrow 0$  for  $x > x^*$ . Then Eq. (4) reduces to the step-function expression, Eq. (7). Note however that  $\lim_{\beta \rightarrow \infty} e^{\beta x^*} I(\beta) = 1/2$  not  $3/2\beta$ , as would be found by naively inserting the limiting density, Eq.(7), in Eq.(3). This means that the dominant contribution to  $I$  is due to the interval

$[0, x^*]$ , even in the limit  $\beta \rightarrow \infty$ , which is readily seen if we write Eq.(6), for large  $\beta$ , as

$$p_{st}(x) \simeq \frac{3}{2}[\Theta(x - x^*) + \Theta(x^* - x)e^{\beta(x-x^*)}] . \quad (8)$$

In the limit  $\beta \rightarrow \infty$ , sites with  $x < x^*$  constitute a set of probability zero, but the site  $m$  selected for extinction belongs to this set *with probability one*. This is a singular property of the Bak-Sneppen model in the infinite-size limit, as discussed in the next subsection. (The infinite-size limit is implicit in mean-field theory.)

Although in the modified models we are unable to find an analytical solution for finite  $\beta$ , it is possible to integrate the mean-field equation numerically. Due to the factor  $e^{\beta x}$ , for large  $\beta$ , a very small time step would be needed to avoid instability in the usual integration methods (e.g., Euler or Runge-Kutta). We circumvent this difficulty using a partial integration method [21]. To apply this method to the MF equation for the original model, we write Eq. (2) in the form

$$\frac{dp(x, t)}{dt} = -f(t)p(x, t) + g(t) , \quad (9)$$

where  $f(t) = e^{-\beta x} + 2I(t)$  and  $g(t) = 3I(t)$ . The formal solution is

$$p(x, t) = \exp\left[-\int_0^t du f(u)\right] \left\{ p(x, 0) + \int_0^t dt' \exp\left[\int_0^{t'} dt'' f(t'')\right] g(t') \right\} . \quad (10)$$

For a small time interval  $\Delta t$ , we find

$$\begin{aligned} p(x, \Delta t) &\simeq e^{-f(0)\Delta t} \left\{ p(x, 0) + g(0) \int_0^{\Delta t} dt' e^{f(0)t'} \right\} \\ &= e^{-f(0)\Delta t} p(x, 0) + \frac{g(0)}{f(0)} (1 - e^{-f(0)\Delta t}) . \end{aligned} \quad (11)$$

This relation can be iterated to find the evolution of  $p(x, t)$  from a given initial distribution, which converges to the stationary density.

## B. BS model on a finite complete graph

Mean-field theory is exact for the “random neighbor” model, which may also be thought of as the BS model on a complete graph, i.e., one in which all pairs of sites are neighbors. (When  $x_m$  is updated, two of these neighbors are chosen at random for updating as well.) In this subsection we analyze the BS model with extremal dynamics on a complete graph of  $N$  sites.

Since sites are assigned independent random numbers, the  $x_i$  are independent, identically distributed random variables drawn from the density  $p(x, t)$ . Define the *distribution function*  $P(x, t) = \int_0^x p(y, t) dy$ . The probability that the next site to be updated,  $x_m$ , lies between zero and  $x$  is:

$$\text{Prob}[x_m \leq x] = 1 - [1 - P(x)]^N, \quad (12)$$

i.e., one less the probability that the minimum is larger than  $x$ . The probability that a randomly chosen neighbor has  $x_i \leq x$  is simply  $P(x)$ , and the probability that one of the updated sites receives a number  $\leq x$  is  $x$ . At each step, therefore, the expected change in the number of sites with  $x_i \leq x$  is  $3x - 2P(x) - \text{Prob}[x_m \leq x]$ , which implies

$$\frac{dP(x, t)}{dt} = -\{1 - [1 - P(x)]^N\} - 2P(x) + 3x. \quad (13)$$

(Here we have taken the time unit to represent  $N$  updates.)

Letting  $Q \equiv 1 - P$ , we have in the stationary state,

$$Q^N + 2Q - 3(1 - x) = 0. \quad (14)$$

(Note that  $Q(0) = 1$ ,  $Q(1) = 0$ , and  $dQ/dx \leq 0$ .) Numerical solution (Fig. 2) shows that for large  $N$ ,  $P_N(x)$  approaches a singular function that is zero for  $x < 1/3$ , while for  $x > 1/3$ ,  $P(x) = 3(x - 1/3)/2$ . It is straightforward to show that for fixed  $x$  and  $N \rightarrow \infty$ ,

$$P(x) \simeq \begin{cases} 1 - (1 - 3x)^{1/N}, & x < 1/3 \\ \frac{3x-1}{2} + \frac{1}{2}[\frac{3}{2}(1-x)]^N, & x > 1/3. \end{cases} \quad (15)$$

For  $x = 1/3$  we have  $\ln P \simeq -\ln N + \ln \ln(N/2)$  (plus terms of lower order in  $N$ ) as  $N \rightarrow \infty$ . Of interest is the exponential convergence of  $P$  to its limiting form for  $x > 1/3$ , compared with algebraic convergence for  $x < 1/3$ . Note also that  $\text{Prob}[x_m \leq 1/3] \simeq 1 - 2/N$ , so that the minimum indeed belongs to the excluded region with probability one, when  $N \rightarrow \infty$ .

### C. Pair approximation

The analysis of the finite-temperature model is readily extended to the pair level, in which one studies the evolution of the two-site joint probability density  $p(x, y)$ . Our starting point is the following exact relation, obtained using the same reasoning that led to Eq. (1):

$$\begin{aligned} \frac{dp(x, y)}{dt} = & -\left(e^{-\beta x} + e^{-\beta y}\right) p(x, y) - \int_0^1 e^{-\beta u} [p(x, y, u) + p(u, x, y)] du \\ & + \int_0^1 \int_0^1 \left(e^{-\beta u} + e^{-\beta v}\right) p(u, v) dudv \\ & + \int_0^1 \int_0^1 [p(x, u, v) + p(v, u, y)] e^{-\beta v} dudv. \end{aligned} \quad (16)$$

Now invoking the pair factorization,

$$p(x, y, u) \simeq \frac{p(x, y)p(y, u)}{p(y)}, \quad (17)$$

Eq. (16) becomes

$$\begin{aligned} \frac{dp(x, y)}{dt} = & - \left[ e^{-\beta x} + e^{-\beta y} + K(x) + K(y) \right] p(x, y) + 2I \\ & + \int_0^1 [p(x, u) + p(y, u)] K(u) du , \end{aligned} \quad (18)$$

with

$$K(x) = J(x)/p(x), \quad (19)$$

$$J(x) = \int_0^1 p(x, u) e^{-\beta u} du \quad (20)$$

and

$$I = \int_0^1 p(x) e^{-\beta x} dx = \int_0^1 J(x) dx . \quad (21)$$

To find the stationary solution numerically, we note that

$$p(x, y) = \frac{2I + \int_0^1 [p(x, u) + p(y, u)] K(u) du}{e^{-\beta x} + e^{-\beta y} + K(x) + K(y)}. \quad (22)$$

Starting from an arbitrary normalized density  $p_0$  (for example, uniform on  $[0, 1] \times [0, 1]$ ), we generate  $p_1$  by evaluating the r.h.s. of Eq. (22) using  $p_0$  and normalizing the resulting expression. This procedure is then iterated until it converges to the stationary density. We find that for large  $\beta$ , the stationary marginal density approaches the step-function solution

$$p(x) = \frac{1}{1 - x^*} \Theta(x - x^*) \Theta(1 - x) \quad (23)$$

with  $x^* \simeq 0.47186$ , a considerable improvement over the site approximation. In this limit, the joint distribution is the product of two identical one-site distributions. Once again, the portion of the unit square that has probability zero is in fact responsible for all transitions. In the region  $D \equiv \{(x, y) | 0 < x, y < x^*\}$ , the two variables are correlated, as shown by the nonzero correlation coefficient  $\rho \equiv \text{cov}(x, y) / \sqrt{\text{var}(x)\text{var}(y)}$ . In the pair approximation,  $\rho \simeq 0.327$  for  $(x, y) \in D$ , as  $\beta \rightarrow \infty$ .

#### D. Radical Variant

In the radical model, the probability density  $p(x) = p_X(x)$  satisfies:

$$\begin{aligned} \frac{dp_X(x)}{dt} = & -e^{\beta x} p_X(x) - 2 \int_0^1 e^{\beta y} p_X(x, y) dy + \int_0^1 e^{\beta y} p_X(y) dy \\ & + 2p_{X^{1/2}}(x) \int_0^1 e^{\beta y} p_X(y) dy , \end{aligned} \quad (24)$$

where  $p_{X^{1/2}}(x) = 2xp_X(x^2)$ . With the definition  $I(\beta) \equiv \int_0^1 e^{\beta y} p(y) dy$  and the mean-field assumption  $p(x, y) = p(x)p(y)$ , Eq. (24) reduces to

$$\frac{dp(x)}{dt} = -e^{\beta x} p(x) + I(\beta)[-2p(x) + 1 + 4xp(x^2)] . \quad (25)$$

Given the step-function form of the stationary density for the original model, it is reasonable to expect that in this case as well,  $p(x)$  will have a jump discontinuity for  $\beta \rightarrow \infty$ , and be zero for  $x > x^*$ . We can get some insight into the nature of the density as  $\beta \rightarrow \infty$  by first observing that if  $p(x) \leq C < \infty$  as  $x \rightarrow 1$ , then  $I \sim Ce^\beta/\beta$  for large  $\beta$ , and therefore  $e^{-\beta}I \rightarrow 0$  as  $\beta \rightarrow \infty$ . This in fact holds unless  $p(x)$  has a  $\delta$ -like contribution at  $x = 1$ , which is not expected since it is precisely the largest values of  $x$  that are removed in the dynamics. Write the stationary solution to Eq. (25) as

$$p(x) = \frac{\bar{I}[1 + 4xp(x^2)]}{1 + 2\bar{I}} , \quad (26)$$

with  $\bar{I} = e^{-\beta x}I$ . This gives  $p(1) = 0$  in the limit  $\beta \rightarrow \infty$ . Similarly, supposing that  $xp(x^2) \rightarrow 0$  as  $x \rightarrow 0$ , we have  $p(0) = 1/2$  in this limit. A similar line of reasoning can be used to show that  $dp/dx|_{x=1} = 0$  in the  $\beta \rightarrow \infty$  limit.

The preceding discussion suggests that in the limit  $\beta \rightarrow \infty$ ,  $p_{st}(x)$  is *identically zero* over some finite range  $[x^*, 1]$ . Assuming this to be so, we have  $I \sim e^{\beta x^*}$  and in the limit  $\beta \rightarrow \infty$  the stationary solution is given by the *functional equation*:

$$2p(x) - 4xp(x^2) = 1 , \quad (27)$$

for  $0 \leq x < x^*$ . Writing this as  $p(x) = 1/2 + 2xp(x^2)$ , we can iterate to find  $p(x^2) = 1/2 + 2x^2p(x^4)$ ,  $p(x^4) = 1/2 + 2x^4p(x^8)$ ,  $p(x^8) = 1/2 + 2x^8p(x^{16})$ , etc., which suggests the solution

$$p_1(x) = \frac{1}{2} + x + 2x^3 + 4x^7 + 8x^{15} + \dots = \sum_{i=0}^{\infty} 2^{i-1} x^{2^i-1} . \quad (28)$$

Substituting this ‘lacunary series’ in Eq.(27), one readily verifies that  $p_1(x)$  is a solution. Similarly, rewriting Eq.(27) as  $p(x^2) = -1/4x + p(x)/2x$ , one finds  $p(x) = -1/4x^{1/2} + p(x^{1/2})/2x^{1/2}$ ,  $p(x^{1/2}) = -1/4x^{1/4} + p(x^{1/4})/2x^{1/4}$ , etc., leading to a second solution:

$$p_2(x) = -\frac{1}{4x^{1/2}} - \frac{1}{8x^{3/4}} - \frac{1}{16x^{7/8}} - \frac{1}{32x^{15/16}} - \dots = -\sum_{i=1}^{\infty} 2^{-(i+1)} x^{-(1-2^{-i})} . \quad (29)$$

We now search a solution of the form  $p(x) = Ap_1(x) + Bp_2(x)$ ; substituting in Eq. (27), yields the condition  $A + B = 1$ . This linear combination must however be normalizable. The relevant integrals are:

$$\int_0^{x^*} p_1(x)dx = \frac{1}{2} \sum_{n=0}^{\infty} x^{*2^n} = \frac{1}{2}(x^* + x^{*2} + x^{*4} + x^{*8} + \dots) \quad , \quad (30)$$

$$\int_0^{x^*} p_2(x)dx = -\frac{1}{2} \sum_{n=1}^{\infty} x^{*2^{-n}} = -\frac{1}{2}(1 + x^{*1/2} + x^{*1/4} + x^{*1/8} + \dots) \quad . \quad (31)$$

Since  $0 < x^* < 1$ , the first integral converges while the second diverges, so that  $p_2(x)$  is not normalizable, implying  $B = 0$ . A normalized, positive solution is  $p(x) = p_1(x)$  for  $x < x^* = 0.793189$  and  $p(x) = 0$  for  $x > x^*$ . ( $x^*$  is determined by normalization.) This solution, for infinite  $\beta$ , is plotted in Fig. 3. Numerical integration of Eq. (25) through the method outlined in Sec. IIIA yields results consistent with this solution, as may again be seen in the figure. Finally, simulation of the random-neighbor version of the model yields a stationary distribution consistent with this expression (see Fig. 4).

We will now analyze the radical model on a finite complete graph and show that its probability density (equation 28) can be derived via a different path. Define the distribution function  $Q(x, t) = \int_x^1 p(y, t)dy$ . By the same reasoning developed in section III B, the probability that  $x_m$ , the next site to be updated, lies between  $x$  and 1 is

$$\text{Prob}[x_m \geq x] = 1 - [1 - Q(x)]^N \quad . \quad (32)$$

The probability that a randomly chosen neighbor has  $x_i \geq x$  is  $Q(x)$ , while the probability that a neighbor receives a barrier  $\geq x$  is  $Q(x^2)$ . The probability that  $x_m$  receives a new value between  $x$  and 1 is simply  $1 - x$ . The expected change in the number of sites with  $x_i \geq x$  is  $(1 - x) + 2Q(x^2) - 2Q(x) - \{1 - [1 - Q(x)]^N\}$ , so that

$$\frac{dQ(x, t)}{dt} = (1 - x) + 2Q(x^2) - 2Q(x) - \{1 - [1 - Q(x)]^N\} \quad . \quad (33)$$

In the stationary state, the definition  $P \equiv 1 - Q$  leads to

$$x + 2P(x^2) - 2P(x) - P(x)^N = 0 \quad . \quad (34)$$

(Note that  $P(0) = 0$  and  $P(1) = 1$ ). Since  $0 \leq P(x) < 1$  for  $x < x^*$ ,  $\lim_{N \rightarrow \infty} P(x)^N = 0$  and the probability density in an infinite system obeys the functional equation  $x + 2P(x^2) - 2P(x) = 0$ . Using the iterative approach, we find two solutions, one divergent (which is rejected), and the finite solution

$$P(x) = \frac{1}{2} \sum_{n=0}^{\infty} x^{2^n} \quad , \quad (35)$$

i.e., the integral of  $p_1(x)$ , Eq. (28). Normalization then demands that  $P = 1$  for  $x \geq x^*$ .

Numerical solution of equation (33) (see Fig. 5) shows that, for large  $N$ ,  $P_N(x)$  approaches the singular function described above. For fixed  $x > x^{*1/2}$ , and  $N \rightarrow \infty$ , we find  $P(x) \simeq 1 - x^{1/N}$ .

### E. Centered Square Variant

The probability density in the finite-temperature version of the centered square variant obeys:

$$\frac{dp_X(x)}{dt} = -e^{\beta x} p_X(x) - 2 \int_0^1 e^{\beta y} p_X(x, y) dy + 2 \int_0^1 e^{\beta y} p_X(y) dy + \frac{e^{\beta \sqrt{x}}}{2\sqrt{x}} p_X(\sqrt{x}) . \quad (36)$$

Mean-field factorization leads to

$$\frac{dp(x)}{dt} = -e^{\beta x} p(x) - 2I(\beta)[p(x) - 1] + \frac{e^{\beta \sqrt{x}}}{2\sqrt{x}} p(\sqrt{x}) , \quad (37)$$

with  $I(\beta)$  as defined in Sec. IIID. In the stationary state, we find

$$p(x) = \frac{2 + \frac{1}{2\sqrt{x}} p(\sqrt{x}) e^{\beta \sqrt{x}} / I}{2 + e^{\beta x} / I} . \quad (38)$$

The hypothesis that in the limit  $\beta \rightarrow \infty$ , the stationary density  $p(x) = 0$  for  $x > x^*$  implies  $I(\beta) \sim e^{\beta x^*}$ . Therefore

$$\lim_{\beta \rightarrow \infty} \frac{e^{\beta x}}{I} = \begin{cases} 0 & \text{if } x < x^* \\ \infty & \text{if } x > x^* \end{cases} \quad (39)$$

and

$$\lim_{\beta \rightarrow \infty} \frac{e^{\beta \sqrt{x}}}{I} = \begin{cases} 0 & \text{if } x < x^{*2} \\ \infty & \text{if } x > x^{*2} \end{cases} \quad (40)$$

This, combined with Eq. (38), implies that  $p(x) = 1$  for  $x \in [0, x^{*2}]$ , and that

$$p(x) = \lim_{\beta \rightarrow \infty} \left[ 1 + \frac{1}{4\sqrt{x}} \frac{e^{\beta \sqrt{x}}}{I} p(\sqrt{x}) \right] \quad \text{for } x \in [x^{*2}, x^*] \quad (41)$$

The iterative process used in the preceding section is not useful here as it leads to pathological solutions, due to the divergent ratio  $e^{\beta \sqrt{x}}/I$  in this interval. Observe that if, for  $x \in [x^*, x^{*1/2}]$ ,  $p(x) = g(x^2)I/e^{\beta x}$ , as  $\beta \rightarrow \infty$ , with  $g(x^2)$  finite, then  $p(x) = 1 + g(x)/4\sqrt{x}$  for  $x \in [x^{*2}, x^*]$ . (Note that this means that  $p(x) \rightarrow 0$  as  $\beta \rightarrow \infty$  for  $x$  in the interval  $[x^*, x^{*1/2}]$ , consistent with the hypothesis that  $p(x) \rightarrow 0$  for  $x > x^*$ .) The function  $g(x)$  is however yet to be determined. Attempting the simplest solution,  $g(x) = \text{constant}$ , we find a surprisingly reasonable result, as shown in Fig. 6. Next, allowing  $g(x) = ax + b$ , with  $a$  and  $b$  constant, yields excellent agreement with the numerical integration of Eq. (37) as also shown in Fig. 6. We do not have an argument why  $g(x)$  should take this form.

The threshold  $x^*$  can be determined in a simple way. Since the fraction of barriers in the interval  $[x^*, 1]$  is constant in the stationary state, the mean number of barriers removed from this interval at each time step must equal the mean number inserted. The probability that the maximum  $x_M$  lies in  $[x^*, 1]$  is 1, while its random neighbors are certainly below  $x^*$ . Each updated neighbor has a probability  $(1 - x^*)$  of receiving a barrier in the interval  $[x^*, 1]$ , while the maximum remains in  $[x^*, 1]$  with probability  $p_1$ , the probability that  $x_M \in [x^{*1/2}, 1]$ . Thus, we have

$$1 = 2(1 - x^*) + p_1 \quad . \quad (42)$$

This reasoning can be repeated for the intervals  $[x^{*1/2}, 1]$ ,  $[x^{*1/4}, 1]$ , ..., leading to

$$p_1 = 2(1 - x^{*1/2}) + p_2 \quad , \quad (43)$$

$$p_2 = 2(1 - x^{*1/4}) + p_3 \quad \dots \quad (44)$$

where  $p_n$  is the probability that  $x_M \in [x^{*1/2^n}, 1]$ . Substituting this result in equation (42), we find

$$1 = 2(1 - x^*) + 2(1 - x^{*1/2}) + 2(1 - x^{*1/4}) + 2(1 - x^{*1/8}) + \dots \quad , \quad (45)$$

which provides  $x^* = 0.761072$ . Finally, we note that normalization implies  $\int_{x^*}^1 g(x)/4\sqrt{x} dx = 1 - x^* = 0.238928$ , providing a constraint on the function  $g(x)$ .

## F. Peripheral Square Variant

We now apply the mean-field analysis to the peripheral square variant. In this case, the probability density satisfies:

$$\begin{aligned} \frac{dp_X(x)}{dt} = & -e^{\beta x} p_X(x) - 2 \int_0^1 e^{\beta y} p_X(x, y) dy + 2 \int_0^1 e^{\beta y} p_X(y) dy \\ & + p_{X^2}(x) \int_0^1 e^{\beta y} p_X(y) dy \quad , \end{aligned} \quad (46)$$

where  $p_{X^2}(x) = p_X(x^{1/2})/2x^{1/2}$ . Under the mean-field factorization this reduces to

$$\frac{dp(x)}{dt} = -e^{\beta x} p(x) + I(\beta)[-2p(x) + 2 + \frac{1}{2x^{1/2}}p(x^{1/2})] \quad , \quad (47)$$

with  $I(\beta)$  as given in Sec. IIIC. The hypothesis that, for  $\beta \rightarrow \infty$ , the stationary density  $p(x) = 0$  for  $x > x^*$  implies  $I(\beta) \sim e^{\beta x^*}$ , leading to the functional equation:

$$p(x) - \frac{1}{4x^{1/2}}p(x^{1/2}) = 1 \quad (\beta \rightarrow \infty) \quad , \quad (48)$$

for  $x < x^*$ .

As in the centered-square variant, the iterative method does not yield a useful solution, and we pursue a different approach. Let  $p(x) = f(x)$  on the interval  $x^{*2} \leq x < x^*$ , where the function  $f(x)$  and the constant  $x^*$  are yet to be determined. Using Eq. (48), we find that

$$p(x) = 1 + \frac{f(x^{1/2})}{4x^{1/2}} \quad \text{for } x^{*4} \leq x < x^{*2} \quad , \quad (49)$$

$$p(x) = 1 + \frac{1}{4x^{1/2}} + \frac{f(x^{1/4})}{4^2 x^{3/4}} \quad \text{for } x^{*8} \leq x < x^{*4} \quad , \quad (50)$$

$$p(x) = 1 + \frac{1}{4x^{1/2}} + \frac{1}{4^2 x^{3/4}} + \frac{f(x^{1/8})}{4^3 x^{7/8}} \quad \text{for } x^{*16} \leq x < x^{*8} \quad , \text{ etc.} \quad (51)$$

Thus we have found a family of solutions  $p(x)$  to Eq.(48), which is quite general since  $f(x)$  is still undetermined.

We now show that  $f(x) = 1$  on the interval  $[x^{*2}, x^*)$ . To begin, we note that in the stationary state, Eq. (47) implies

$$\left( \frac{e^{\beta x}}{I} + 2 \right) p(x) = 2 + \frac{p(\sqrt{x})}{2\sqrt{x}} \quad . \quad (52)$$

In particular, for  $x = 1$  we have

$$\left( \frac{e^{\beta}}{I} + \frac{3}{2} \right) p(1) = 2 \quad , \quad (53)$$

so that if  $I \simeq Ae^{\beta x^*}$ , then  $p(1) \simeq 2Ae^{-\beta(1-x^*)}$ . It is readily seen that  $p(x) \simeq 2Ae^{-\beta(x-x^*)}$  satisfies Eq. (52) for  $x^* < x \leq 1$ . The same equation then leads to  $p(x) = 1$  as  $\beta \rightarrow \infty$ , for  $x^{*2} < x < x^*$ . We may then develop the full solution using Eqs. (49) to (51); normalization implies  $x^* = 1/2$ . The result is the function  $p(x)$  plotted in Fig. 7, which is in good agreement with the density found via simulation of the random-neighbor model. This solution is discontinuous at  $x^*$ ,  $x^{*2}$ ,  $x^{*4}$ , ..., and exhibits an integrable divergence at  $x = 0$ .

The value of  $x^*$  can be confirmed through the reasoning developed in previous subsection for the peripheral square model, which in this case implies  $1 = 2(1 - x^*)$  so that  $x^* = 1/2$ .

#### IV. NUMERICAL SIMULATION AND CRITICAL EXPONENTS

We now compare the mean-field theory predictions with simulation results. We estimate the probability density  $p(x)$  on the basis of a histogram of barrier frequencies, dividing  $[0,1]$  into 100 subintervals. Histograms are accumulated after  $N_{st}$  time steps, as required for the system (a ring of  $N$  sites) to relax to the stationary state. In order to improve statistics, we average over  $N_r$  realizations.

The simulation results for the original BS model are shown in Fig. 8. We observe qualitative agreement between nearest-neighbor (NN) and random-neighbor (RN) versions. (The simulation parameters are:  $N = 1000$ ,  $N_{st} = 10^6$ ,  $N_r = 10^3$  (NN);  $N = 2000$ ,  $N_{st} = 10^5$ ,  $N_r = 10^3$  (RN).) Here and in all other cases, the simulation result for the random neighbor model appears to converge (as expected) to the mean-field prediction. In light of the discussion in Sec. IIIB, it is reasonable to regard the rounding of the step function as a finite-size effect.

Fig. 4 presents similar results for the radical variant. We notice that the NN and RN versions exhibit qualitatively similar probability densities, differing mainly in the value of the threshold  $x^*$ . (In this case we use  $N_{st} = 10^6$  and  $N_r = 10^3$ , with system sizes  $N = 1000$  (NN) and  $2000$  (RN).)

Simulation results for the centered and peripheral square versions are shown in Fig. 9 and 10, resp.. For the centered square, the NN and RN, probability densities are quite similar, differing mainly in the value of the threshold and in the inclination of the central portion (Fig. 9). (The simulation parameters are  $N = 2000$ ,  $N_{st} = 10^7$ ,  $N_r = 500$  (NN),  $N = 10000$ ,  $N_{st} = 10^6$ ,  $N_r = 10^3$  (RN).) On the other hand, for the peripheral square version, the nearest-neighbor and random-neighbor densities are somewhat different, since the latter exhibits various steps, while only one such step is evident in the former (see Fig. 10). Further study is needed to determine whether this represents a qualitative difference between the two formulations, or is instead due to finite size and/or finite numerical resolution. (Note that for the square models we use larger lattices, which were necessary to observe clear singularities. The simulation parameters are:  $N = 1000$ ,  $N_{st} = 10^6$ ,  $N_r = 10^3$  (NN),  $N = 50000$ ,  $N_{st} = 10^7$ ,  $N_r = 20$  (RN).)

Several quantities are known to display power-law behaviour in the Bak-Sneppen model [1,6,18]. In particular, we studied the distribution  $P_J(r)$  that successive updated sites are separated by a distance  $r$ . In the original model,  $P_J(r) \sim r^{-\pi}$ , with  $\pi = 3.23(2)$  [18]. (Figures in parentheses denote uncertainties.) We performed simulations of the modified models using  $10^9$  time steps on lattices of 2000 or more sites, yielding (see Fig. 11),  $\pi = 3.22(2)$  for the original BS model;  $\pi = 3.27(2)$  for the radical variant;  $\pi = 3.25(2)$  and  $3.24(2)$  for the centered and peripheral square variants, respectively. Thus we find strong evidence that all of the variants introduced here belong to the same universality class as the original model.

## V. CONCLUSIONS

In order to understand the implications of extremal dynamics, we propose several modified Bak-Sneppen models. Although different updating rules lead to completely different probability densities, they are always singular at one or more points. The step-like singularities appear in the limiting densities, either as  $\beta \rightarrow \infty$  in the finite temperature model (on an infinite lattice), or as the system size  $N \rightarrow \infty$ , under extremal dynamics. Thus the double limit of

infinite size and zero temperature is required for the BS model or its variants to generate a singular probability density.

A remarkable feature common to the original model and all the variants considered, is that in the infinite-size limit, and under extremal dynamics, a certain interval  $D \subset [0, 1]$  has probability zero, and yet contains the extremal site with probability one. If we regard the density of active sites,  $\text{Prob}[x \in D]$ , as the order parameter  $\rho$ , then the BS model and its variants are seen to realize the ‘SOC limit’ [4,5]  $\rho \rightarrow 0^+$ . Correlations between site variables  $x_i, x_j, \dots, x_n$  are zero unless one or more of these values falls in  $D$ .

Our conclusions regarding the form of the stationary densities are based on mean-field analyses that are exact for the random-neighbor versions, as is verified numerically. We also present a pair approximation for the original model. An important point is that mean-field theory captures the form of the probability density correctly, as shown via simulations of the modified models on a one-dimensional lattice. The latter suggest that the critical exponents are independent of dynamics.

The Bak-Sneppen model appears to be a prototype for a large universality class, since countless variants, beyond those presented here, are possible. We expect any dynamics that respects the symmetry of the original model (that is, spatial isotropy), and that does not introduce new conserved quantities, to have the same exponents as the original model. This is interesting, since the same critical behavior may subsist, as it were, upon stationary distributions of very different forms. Aside from its intrinsic interest, the question of universality is important for applications, since the precise form of the dynamics in a specific setting (e.g., evolution) is generally unknown, and probably quite different from that of the original model. Power laws and a singular stationary density only appear in the extremal dynamics limit, which may be difficult to realize in spatially extended natural systems.

## ACKNOWLEDGMENTS

We thank CNPq and CAPES, Brazil, for financial support.

## REFERENCES

- [1] P. Bak, K. Sneppen, Phys. Rev. Lett. 71 (1993) 4083.
- [2] R. Donangelo, H. Fort, Phys. Rev. Lett. 89 (2002) 038101.
- [3] I. Bose, I. Chaudhuri, Int. J. Mod. Phys. C 12 (2001) 675.
- [4] R. Dickman, M.A. Muñoz, A. Vespignani, S. Zapperi, Braz. J. Phys. 30 (2000) 27.
- [5] D. Head, Eur. Phys. J. B 17 (2000) 289.
- [6] P. Grassberger, Phys. Lett. A 200 (1995) 277.
- [7] P.D. Rios, M. Marsili, M. Vendruscolo, Phys. Rev. Lett. 80 (1998) 5746.
- [8] S. Boettcher, M. Paczuski, Phys. Rev. Lett. 84 (2000) 2267.
- [9] R. Meester, D. Znamenski, J. Stat. Phys. 109 (2002) 987.
- [10] W. Li, X. Cai, Phys. Rev. E 62 (2000) 7743.
- [11] S.N. Dorogovtsev, J.F.F. Mendes, Y.G. Pogorelov, Phys. Rev. E 62 (2000) 295.
- [12] G. Caldarelli, M. Felici, A. Gabrielli, L. Pietronero, Phys. Rev. E 65 (2002) 046101.
- [13] M. Felici, G. Caldarelli, A. Gabrielli, L. Pietronero, Phys. Rev. Lett. 86 (2001) 1896.
- [14] M. Marsili, Europhys. Lett. 28 (1994) 385.
- [15] B. Mikeska, Phys. Rev. E 55 (1997) 3708.
- [16] M. Paczuski, S. Maslov, P. Bak, Europhys. Lett. 27 (1994) 97.
- [17] Y.M. Pismak, Phys. Rev. E 56 (1997) R1326.
- [18] D.A. Head, G.J. Rodgers, J. Phys. A 31 (1998) 3977.
- [19] S. Maslov, P. De Los Rios, M. Marsili, Y.-C. Zhang, Phys. Rev. E 58 (1998) 7141.
- [20] B. Drossel, Adv. Phys. 50 (2001) 209; e-print: cond-mat/0101409.
- [21] R. Dickman, Phys. Rev. E 65 (2002) 047701.

## FIGURES

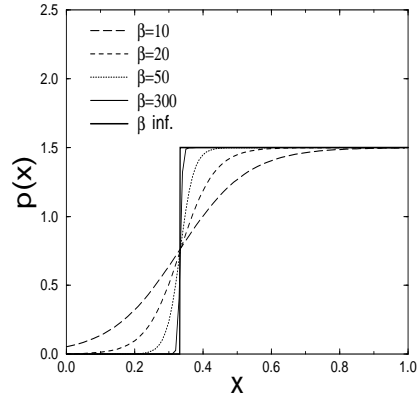


FIG. 1. Original model: finite-temperature mean-field theory Eq. (6) for  $\beta$  values as indicated ( $\beta$  inf. stands for  $\beta \rightarrow \infty$ ).

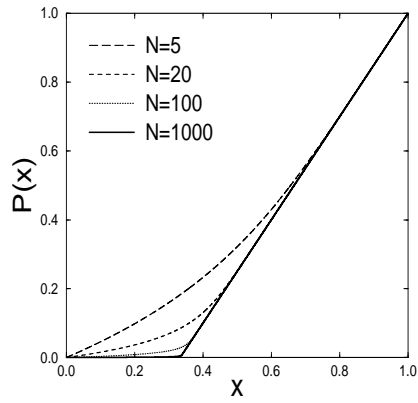


FIG. 2. Original model on complete graph (extremal dynamics) for system sizes as indicated.

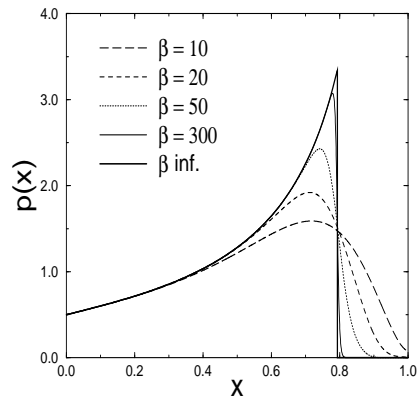


FIG. 3. Radical variant: finite-temperature mean-field theory for  $\beta$  values as indicated.

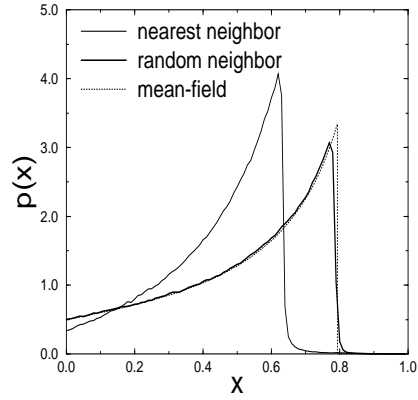


FIG. 4. Radical variant: simulation results for nearest neighbor and random neighbor versions compared with mean-field prediction.

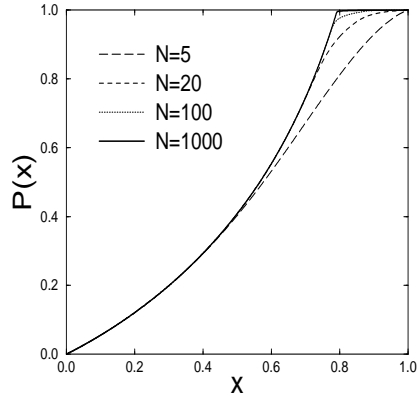


FIG. 5. Radical variant on complete graph for system sizes as indicated.

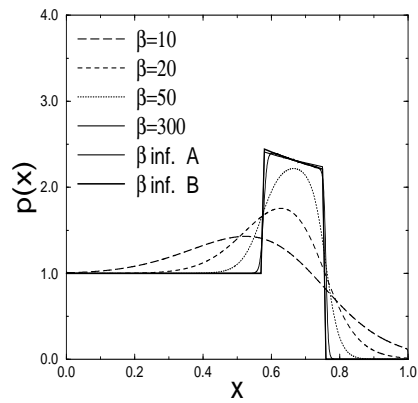


FIG. 6. Centered square variant: finite-temperature mean-field theory for  $\beta$  values as indicated. Approximation A refers to  $g(x) = \text{constant}$ , B for  $g(x) = ax + b$ , both at zero temperature, as explained in text.

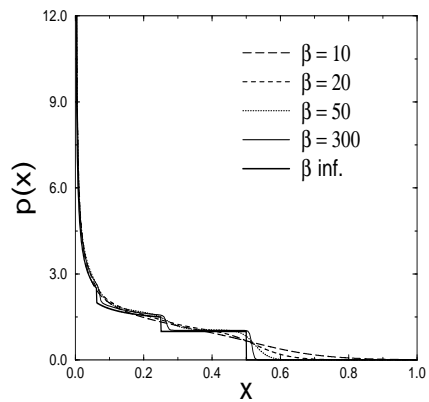


FIG. 7. Peripheral square variant: finite-temperature mean-field theory for  $\beta$  values as indicated.

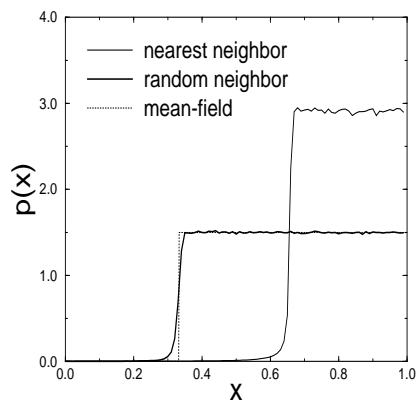


FIG. 8. Original model: simulation results for NN and RN versions compared with mean-field prediction.

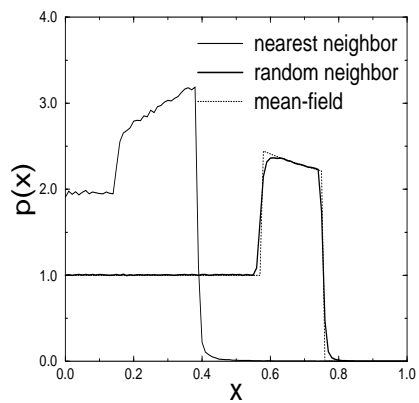


FIG. 9. Centered square variant: simulation results for NN and RN versions compared with mean-field prediction.

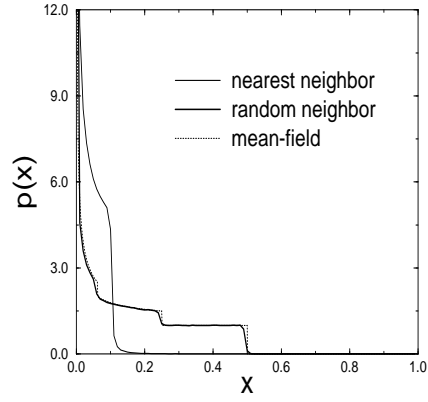


FIG. 10. Peripheral square variant: simulation results for NN and RN versions compared with mean-field prediction.

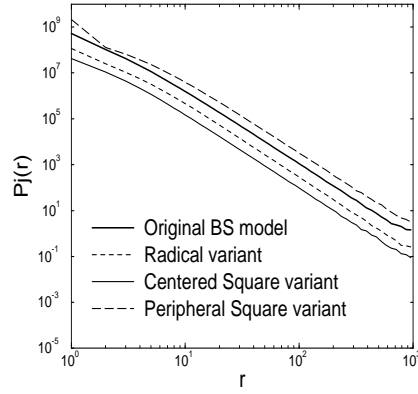


FIG. 11. Distribution  $P_J(r)$  of the distance  $r$  separating successive updated sites. The curves have been shifted vertically to facilitate comparison.